

## **Optimal pipeline design considering failure by mechanical damage**

Felipe Alexander Vargas Bazán

Department of Structural Engineering, University of São Paulo, Brazil

André Teófilo Beck

Department of Structural Engineering, University of São Paulo, Brazil

### **1. INTRODUCTION**

It is nowadays largely recognized that mechanical damage by external interference can represent a serious threat to the structural integrity of high pressure onshore pipelines. International databases [1-3] show that mechanical damage is a major cause of spillage in pipelines. In European gas pipelines [1], external interference is pointed out as the cause of 50% of all incidents. CONCAWE data [2] indicates that third-party activity accounts for 42% of all incidents in European cold oil pipelines. Similarly, UKOPA [3] reports that external interference is the cause of most spillage incidents in UK pipelines.

In onshore (buried) pipelines, mechanical damage is typically due to excavating or hole equipment impact, which may be caused by several agents such as the pipeline operator, service providers, or external agents (third-party damage). External agents include building companies and companies working on ground excavation. Mechanical damage can also be caused by settlement of the buried pipeline over rocks, or by compression of the pipeline body by rocks due to ground movements. Defects caused by mechanical damage can be of different types, such as dents, gouges and cracks. The present article is not concerned with the particular type of mechanical damage defect.

A literature review shows several articles addressing optimal design of pipelines subject to corrosion [4-7], which is also a significant failure mode for buried pipelines. However, no similar articles were found addressing optimal design considering failure by mechanical damage. Zhou & Nessim [5] dealt with the optimal design of onshore natural gas pipelines, comparing ten different wall thicknesses. Besides corrosion, the authors considered equipment impact due to third-party interference as a failure cause. However, inspection costs and optimal inspection schedules related to equipment impact were not considered in [5].

Pipeline systems can be safely designed using conservative design margins. However, when the optimum design of such systems is addressed, usual conservativeness needs to be removed. Moreover, since failures in large pipeline networks are largely unavoidable, expected consequences (costs) of failure also have to be considered [8,9].

The present paper addresses the optimal design of buried pipelines considering failure by mechanical damage. Historical incident data relating failure rates with problem parameters is used to guide the optimization process. The optimal external diameter, depth of cover and surveillance interval are considered as design variables. The design objective is to minimize total lifecycle costs, which include costs of construction, inspections, and expected costs of failure and repair.

The remainder of this article is structured as follows. The methodology employed to estimate failure rates, based on historical failure data, is described in Section 2. Section 3 describes the optimization problem and the objective function. Results of a numerical application are presented and discussed in Section 4. Section 5 presents some concluding remarks.

## 2. ESTIMATE OF FAILURE RATES BASED ON HISTORICAL FAILURE DATA

The design of optimal pipeline systems considering failure by mechanical damage requires estimating failure rate for different pipeline parameters. The failure rate,  $\lambda_f$ , per km·year, of a pipeline due to mechanical damage can be calculated as [10]:

$$\lambda_f = \omega P_f \quad (1)$$

where  $\omega$  is the frequency of impact events, or frequency of hits (impacts per km·year), and  $P_f$  is the probability of failure given the occurrence of an impact, or conditional probability of failure.

The frequency of impact events can be estimated by physical attributes such as land use, depth of cover and use of mechanical protection, as well as by prevention measures such as frequency of right-of-way patrols, one-call systems, public awareness programs and excavation procedures. Chen & Nessim [11] described a fault tree model to calculate the frequency of occurrence of equipment impact events from the frequency of construction activity and the damage mitigation measures implemented for a given pipeline.

The conditional failure probability can be calculated from mechanical damage failure models, e.g. dent-gouge models based on elastic-plastic fracture mechanics [10, 12-16] together with probabilistic models for the involved random quantities [10]. Application of these probabilistic failure models, however, has limitations. An idealized geometry of the damage is heuristically assumed, and probabilistic models are required for variables such as pipe diameter, wall thickness, material properties, internal pressure, gouge dimensions, excavator weight and force, and so on. In addition, empirical models relating the impact force with dent depth are also required.

As an alternative, Goodfellow et al. [17] presented failure rate curves which have been included as supplements in the UK design codes IGE/TD/1 and PD 8010 [18]. These curves were obtained from parametric analysis, using the dent-gouge model [19, 20], and can be compared to historical incident data. These curves are used in the present paper to estimate failure rates, and are briefly described in the following.

A generic failure rate ( $\lambda_0$ ) curve was derived from parametric analyses, with probabilities of failure calculated from the original dent-gouge model [19, 20], for pipelines of different diameters with a constant design factor of 0.72, a constant wall thickness of 5 mm and material grade X65. Figure 1 illustrates the generic failure rate curve for mechanical damage, in terms of pipe external diameter  $D$ . This curve has been “calibrated” to match historical failure rate data. For  $D=200$  mm, for instance, the generic failure rate is 0.223 failures per thousand km·year. Historical failure rates for UKOPA [3] are 0.2, for CONCAWE [2] and for EGIG [1] 0.3 failures per thousand km·year. For larger diameters, generic failure rates obtained directly from Figure 1 are larger than historical rates, because they are further affected by the reduction factors to be presented.

The generic failure rates in Fig. 1 are updated taking into account other problem parameters, such as design factor, wall thickness, depth of cover and surveillance intervals. The effect of these variables is derived from historical failure data. Thus, the total failure rate,  $\lambda_f$ , due to mechanical damage and for a given pipeline, can be estimated from the generic failure rate and the following reduction factors:

$$\lambda_f = \lambda_0 R_{df} R_{wt} R_{dc} R_{si} \quad (2)$$

where  $\lambda_f$  and  $\lambda_0$  are expressed per km·year, and where  $R_{df}$ ,  $R_{wt}$ ,  $R_{dc}$ , and  $R_{si}$  are the non-dimensional reduction factors for design factor, wall thickness, depth of cover and surveillance interval, respectively.

Figures 2 and 3 show reduction factors for design factor ( $R_{df}$ ) and wall thickness ( $R_{wt}$ ), respectively. As explained elsewhere [17, 18], these reduction factors were derived from comprehensive parametric studies [21] carried out using mechanical models describing pipeline failure due to gouge and dent-gouge

damage [19, 20], and historical damage statistics derived from the UKOPA [3] pipeline database. Reduction factors  $R_{df}$  and  $R_{wt}$  are based on a conservative interpretation of the results of the parametric studies. The reduction factor  $R_{wt}$  in Fig. 3 can be qualitatively compared with historical failure rates for UKOPA [3]. Table 1 shows the range of pipeline parameters over which these reduction factors are applicable.

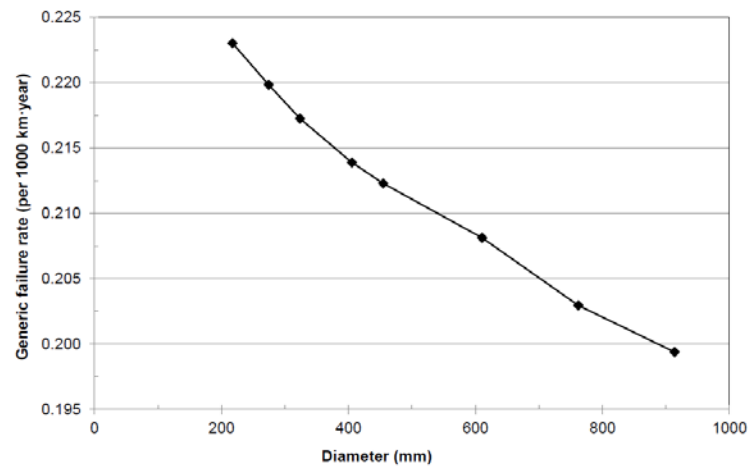


Figure 1 - Generic failure rate due to mechanical damage as a function of pipeline diameter (adapted from PD8010:2009).

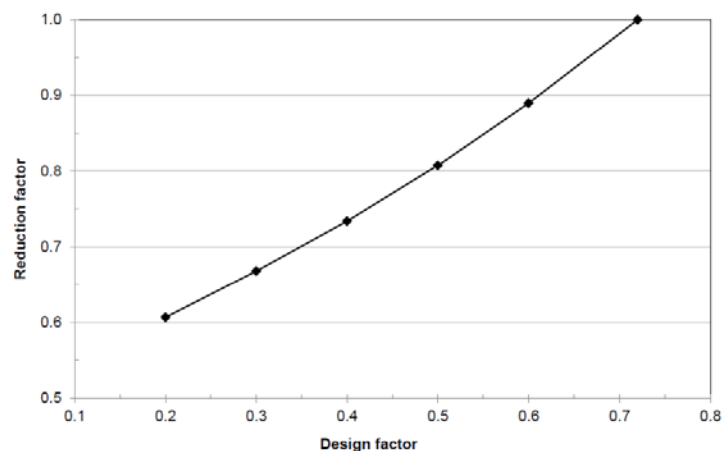


Figure 2 - Reduction in mechanical damage failure rate due to design factor (adapted from PD8010:2009).

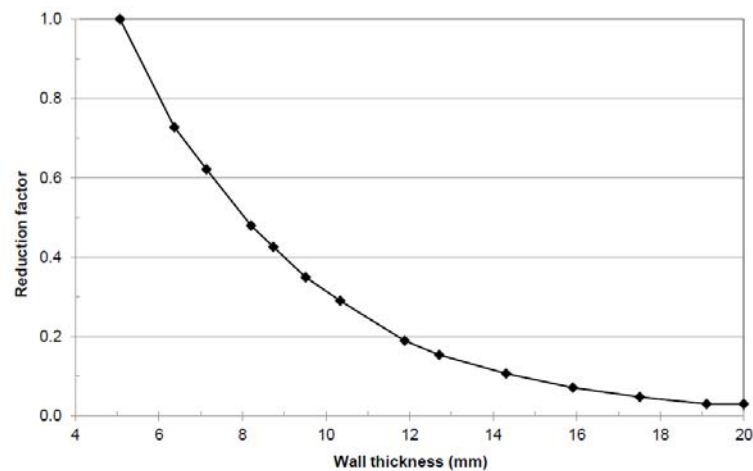


Figure 3 - Reduction in mechanical damage failure rate due to wall thickness for  $\phi=0.72$  (adapted from PD8010:2009).

Table 1: Range of applicability of reduction factor for design factor,  $R_{df}$ , and reduction factor due to wall thickness,  $R_{wt}$  (PD 8010:2009).

Parameter	Range of applicability of $R_{df}$ and $R_{wt}$
Design factor	$\leq 0.72$
Wall thickness	$\geq 5$ mm
Material grade	$\leq X65$
Diameter	219.1 mm to 914.4 mm
Charpy energy	$\geq 24$ J (average)

The reduction factor for depth of cover,  $R_{dc}$ , is shown in Figure 4. These results were derived by Mather et al. [22], and can be compared with historical failure rates reported by EGIG [1]. The reduction factor for surveillance interval,  $R_{si}$ , is shown in Figure 5. According to PD8010:2009 [18], this factor was derived from studies by UKOPA, relating data on infringement incidence to data on damage incidence.

In conclusion, the failure rate of a particular pipeline, due to mechanical damage (external interference), could be estimated using Equation (1) or Equation (2). In this paper, Eq. (2) and Figs. 1 to 5 are employed. The design optimization problem developed in Section 3 can be employed with any valid way of estimating the failure rates. If a reliable, non-conservative failure model were available, its use and the subsequent application of Eq. (1) could be more realistic.

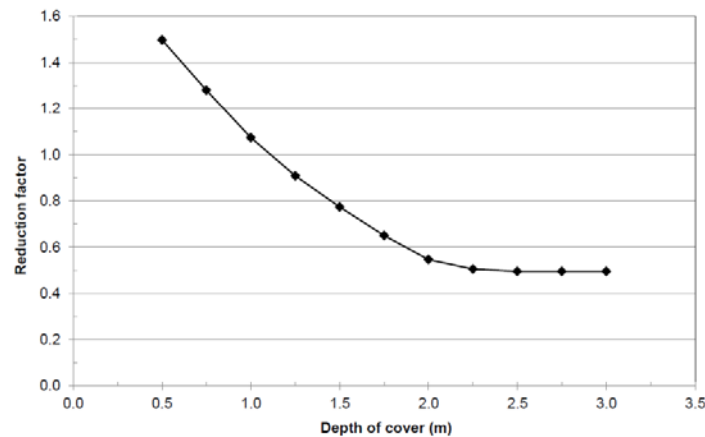


Figure 4 - Reduction in mechanical damage failure rate due to depth of cover (adapted from PD8010:2009).

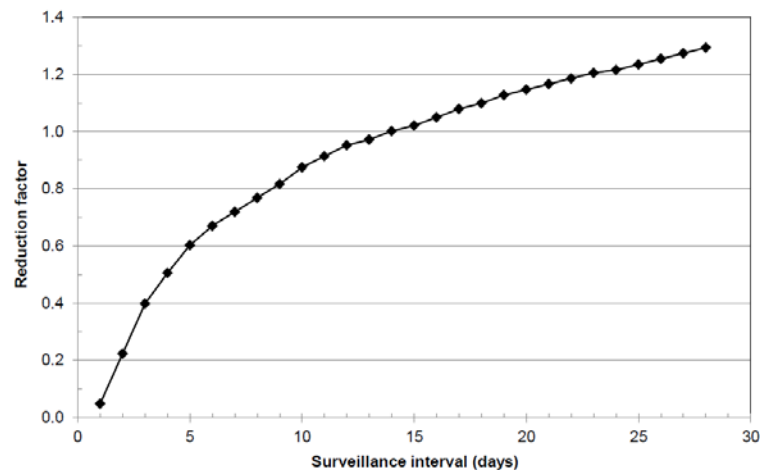


Figure 5 - Reduction in mechanical damage failure rate due to surveillance interval (adapted from PD8010:2009).

### 3. DESIGN OPTIMIZATION PROBLEM

Following Zhou & Nessim [5] and Gomes & Beck [7], in the present article the design optimization problem is solved from an initial design perspective; therefore, the costs of inspection, repair and failure are brought to the design (decision) time, using a proper discount function. The optimization aims to guide the design process, by including initial costs but also considering future expected costs of inspection, failure and repair.

The design variables considered in the optimization problem are the external diameter, depth of cover and surveillance interval.

#### 3.1 Relationship between pipe diameter and design pressure

For a given pipeline, the design factor and volume flow rate of the transported fluid are taken as fixed, given, parameters. The design factor depends on pipeline classification, which is related to

population density and land use in the pipeline site [18, 23]. This classification also takes into account type of fluid transported and other failure modes such as leaks and rupture due to corrosion. The volume flow rate is specified by the owner or end-user of the pipeline.

Hence, we assume that the external diameter is a free design variable. Also, it is known that, for the same flow rate, larger diameters will allow lower internal pressures to be used. The following equation expresses the relationship between internal diameter and internal pressure, for fully developed laminar flow in a horizontal pipe [24]:

$$Q = \frac{\pi \Delta p D_i^4}{128 \mu L} = \frac{\pi (p_1 - p_2) D_i^4}{128 \mu L} \quad (3)$$

In Equation (3),  $Q$  is the volume flow rate of the fluid,  $\Delta p$  is the pressure drop between two points (1 and 2) along the pipe route,  $p_1$  and  $p_2$  are the pressures at these points,  $L$  is the length of pipe segment between the two points,  $D_i$  is the pipe internal diameter, and  $\mu$  is the absolute (or dynamic) viscosity of the fluid. Assuming in Eq. (3), for simplicity, that  $p_1 = p$ , the maximum allowed design pressure (MAOP), and  $p_2 = 0$ , along a reference length  $L$ , one obtains:

$$p = \frac{128 \mu L Q}{\pi D_i^4} = \frac{128 \mu L Q}{\pi (D - 2 w_t)^4} \quad (4)$$

where  $D$  is the pipe (external) diameter, and  $w_t$  is the pipe wall thickness. On the other hand, from the well-known Barlow equation, the pipe wall thickness,  $w_t$ , can be expressed as:

$$w_t = \frac{p D}{2 \phi SMYS} \quad (5)$$

where  $\phi$  is the design factor, and  $SMYS$  is the material specified minimum yield strength. Substituting Equation (5) into Equation (4) results in:

$$p = \frac{128 \mu L Q}{\pi \left( D - \frac{p D}{\phi SMYS} \right)^4} \quad (6)$$

For a given pipe external diameter ( $D$ , which is a design variable in the optimization problem), the design pressure can be calculated by an iterative procedure using Equation (6). Once the design pressure is known, Eq. (5) can be used to calculate the wall thickness.

However, use of Eqs. (5) and (6) without further constraints, leads to pipelines of very large diameter and very small wall thickness. Hence, a further constraint on the  $D/w_t$  ratio needs to be imposed. This constraint, which addresses the susceptibility to flattening, buckling and denting, is usually given by  $D \leq 120 w_t$  [23].

### 3.2 Cost terms

A reference cost ( $C_{ref}$ ) is chosen, from which all other costs are evaluated. The reference cost is the cost of production for a unit-length segment of bare pipe, including transportation and welding, of reference diameter and wall thickness. In the numerical example presented in Section 4, a unitary

reference cost is considered, and all other cost terms are defined as functions of  $C_{ref}$ , using multiplicative factors. All cost terms are evaluated considering one kilometer (1 km) of pipe.

The fabrication cost is the cost of production for a unit-length segment of bare pipe, of given external diameter and wall thickness, including transportation and welding. Since the reference cost is evaluated from reference diameter and wall thickness, the actual fabrication cost,  $C_{pipe}$ , can be evaluated as:

$$C_{pipe}(D, w_t) = f_{pipe}(D, w_t) C_{ref} = \frac{(D/2)^2 - (D/2 - w_t)^2}{(D_r/2)^2 - (D_r/2 - w_{tr})^2} C_{ref} \quad (7)$$

In Equation (7),  $f_{pipe}$  is a multiplicative factor for bare pipe fabrication cost, which is determined as the volume fraction between actual and reference pipe dimensions. An excavation or installation cost,  $C_{exc}$ , is additionally considered:

$$C_{exc} = f_{exc} C_{ref} \quad (8)$$

where  $f_{exc}$  is a multiplicative factor for excavation cost, which is a function of trench depth. The authors could not find, in the published literature, specific information about variation of excavation costs with trench depths. Such information, however, should be easily available to pipeline contractors and operators, who could use more specific information to solve specific problems. In this paper, an empirical function is assumed to describe variation of excavation costs with the depth of cover:

$$f_{exc} = k \sqrt{h} \quad (9)$$

where  $h$  is the depth of cover, and  $k = 0.1 \text{ m}^{-1/2}$  (a constant). Equation (9) is illustrated in Figure 6.

The initial cost of the pipeline,  $C_{ini}$ , is given as the sum of fabrication and excavation costs:

$$C_{ini} = C_{pipe} + C_{exc} = f_{ini} C_{ref} \quad (10)$$

where  $f_{ini} = f_{pipe} + f_{exc}$ .

Cost of surveillance or inspections is given by the surveillance plan. The cost of one inspection occurring at time  $t_v$  is obtained as:

$$C_{insp}^v = f_{insp} C_{ref} e^{-\gamma t_v} \quad (11)$$

where  $f_{insp}$  is a multiplicative factor for inspection cost,  $e^{-\gamma t}$  is a continuous discount function, and  $\gamma$  is the annual discount rate.

Given the design life of the pipeline,  $T$ , and the surveillance interval,  $\Delta_s$ , the number of inspections,  $N_{insp}$ , is:

$$N_{insp} = 1 + \text{floor}\left(\frac{T}{\Delta_s}\right) \quad (12)$$

where  $\text{floor}(\cdot)$  is a function which returns the greatest integer less than or equal to its argument.

The total inspection cost,  $C_{insp\_tot}$ , is simply given by the sum of the costs of each individual inspection:

$$C_{insp\_tot} = \sum_{v=1}^{N_{insp}} C_{insp}^v \quad (13)$$

Note that, for a given surveillance schedule (i.e. for a given value of the design variable  $\Delta_s$ ), the total inspection cost is deterministic, since the time of each inspection and the number of inspections are known from the surveillance interval. Behavior of the total inspection cost with respect to surveillance interval is shown in Figure 7.

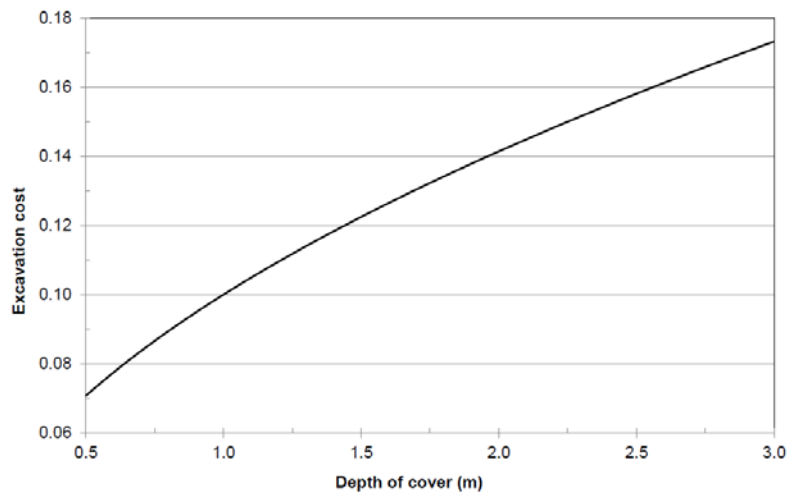


Figure 6 - Variation of excavation cost (factor) with depth of cover.

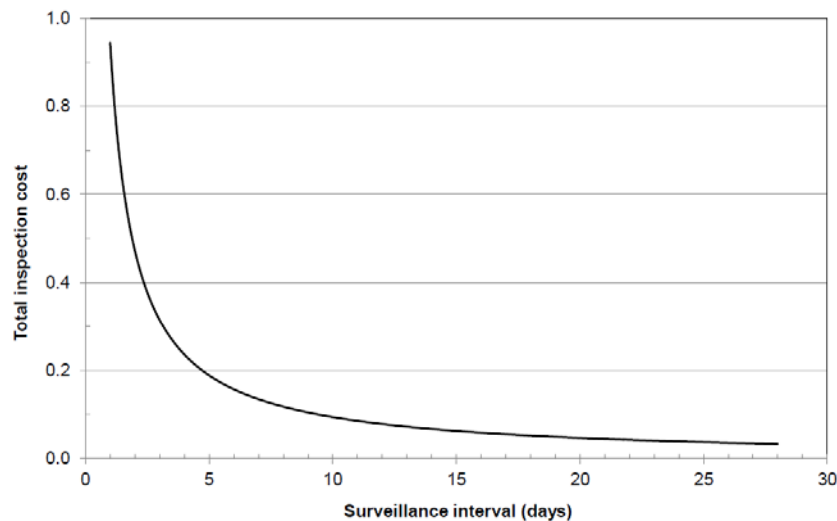


Figure 7 - Total inspection cost as a function of surveillance interval.



The cost of a failure is evaluated as:

$$C_{fail} = f_{fail} C_{ref} E[e^{-\gamma T_{fail}}] \quad (14)$$

where  $f_{fail}$  is a multiplicative factor for failure cost, and  $e^{-\gamma t}$  and  $\gamma$  have the same meanings as in Eq. (11). However, differently from the time at which an inspection occurs, which is deterministic, the time to failure is a random variable, denoted by  $T_{fail}$ . So, in Equation (14) the expected value of the discount function is considered; this is given by:

$$E[e^{-\gamma T_{fail}}] = \frac{\int_0^T f_{T_{fail}}(t) e^{-\gamma t} dt}{\int_0^{T_{fail}} f_{T_{fail}}(t) dt} \quad (15)$$

where  $f_{T_{fail}}(t)$  is the probability density function of the random variable time to failure ( $T_{fail}$ ). This probability density function corresponds to an exponential distribution, and is given by:

$$f_{T_{fail}}(t) = \lambda_f e^{-\lambda_f t} \quad (16)$$

where  $\lambda_f$ , the failure rate, is given by Eqs. (1) or (2).

The expected cost of failure,  $ECF$ , for the pipeline design life  $T$ , is calculated as:

$$ECF = \lambda_f T C_{fail} \quad (17)$$

Not all external interference events lead to immediate failure (pipe rupture). Sometimes, an excavator hits and damages the pipe, causing a dent and a gouge. Depending on the criticality of the damage, and on the knowledge that damage has occurred, pipe operators may decide to repair the damaged pipe. Repair strategies may involve grinding of the gouge root, and/or re-rounding by internal pressurization.

The repair rate is evaluated from the rate of impacts which do not lead to failure. Using conditional failure probabilities, it is possible to calculate the repair rate from the failure rate. From the frequency of impact events,  $\omega$ , and the failure rate,  $\lambda_f$ , the probability of failure given that an impact has occurred,  $P[F|I]$ , can be calculated as:

$$P[F|I] = \frac{\lambda_f}{\omega} \quad (18)$$

Hence, the probability of non-failure, given that an impact has occurred,  $P[NF|I]$ , is:

$$P[NF|I] = 1 - \frac{\lambda_f}{\omega} \quad (19)$$

Denoting by  $\omega_{rep}$  the repair frequency, i.e. the number of dent/gouge defects which are repaired, divided by the total number of dent/gouge defects which do not lead to failure, the probability of repair given that an impact has occurred is obtained as:

$$P[R|I] = \omega_{rep} \left( 1 - \frac{\lambda_f}{\omega} \right) \quad (20)$$

Then, the repair rate (per km·year),  $\lambda_r$ , is calculated as:

$$\lambda_r = P[R|I] \omega = \omega_{rep} (\omega - \lambda_f) \quad (21)$$

On the other hand, similarly to Equation (14), the cost of a repair is evaluated as:

$$C_{rep} = f_{rep} C_{ref} E[e^{-\gamma T_{rep}}] \quad (22)$$

where  $f_{rep}$  is a multiplicative factor for repair cost, and  $e^{-\gamma t}$  and  $\gamma$  have the same meanings as in Eq. (11). In this case the repair time,  $T_{rep}$ , is a random variable. So, in Equation (22) the expected value of the discount function, which is calculated by expressions analogous to Eqs. (15) and (16), is considered. The expected cost of repair,  $ECR$ , for the pipeline design life  $T$ , is calculated as:

$$ECR = \lambda_r T C_{rep} \quad (23)$$

### 3.3 Objective function

The total expected cost, or objective function, is equal to the sum of the initial cost, the total inspection cost, the expected cost of failure, and the expected cost of repair, given by Eqs. (10), (13), (17) and (23), respectively:

$$\begin{aligned} C_{ET}(D, h, \Delta_s) = & C_{ini}(D, h) \\ & + C_{insp\_tot}(\Delta_s) \\ & + \lambda_f(D, h, \Delta_s) T C_{fail} \\ & + \lambda_r(D, h, \Delta_s) T C_{rep} \end{aligned} \quad (24)$$

where the dependence on the design variables was explicitly indicated. The (so-called risk) optimization problem consists of:

$$\begin{aligned} \text{Find : } & (D, h, \Delta_s) \\ \text{which minimizes : } & C_{ET}(D, h, \Delta_s) \\ \text{subject to : } & D \in [D^{\min}, D^{\max}] \\ & h \in [h^{\min}, h^{\max}] \\ & \Delta_s \in [\Delta_s^{\min}, \Delta_s^{\max}] \end{aligned} \quad (25)$$

where  $[D^{\min}, D^{\max}]$ ,  $[h^{\min}, h^{\max}]$  and  $[\Delta_s^{\min}, \Delta_s^{\max}]$  are the lower and upper bounds of the design variables  $D$ ,  $h$  and  $\Delta_s$ , respectively.

## 4. APPLICATION EXAMPLE

### 4.1 Problem description

A hypothetical pipeline was considered to illustrate the optimal design and inspection of onshore pipelines. A design factor ( $\phi$ ) of 0.72 is adopted, which corresponds to a Class 2 gas pipeline [23]. This value of 0.72 comes from the product of a basic design factor of 0.8 by a location factor of 0.9. The pipeline has a design life ( $T$ ) of 50 years. The specified minimum yield strength (SMYS) of the pipe steel is 414 MPa (i.e. X60 steel). To apply Eq. (6), some quantities need to be defined. A reference length ( $L$ ) of 1 km is considered, which is in accordance with the calculated cost terms, all considered per km. The absolute viscosity is  $\mu=0.1$  N·s/m<sup>2</sup>, a typical value for liquefied natural gas (LNG). The volume flow rate is  $Q=5000$  m<sup>3</sup>/h.

The reference cost is taken equal to one ( $C_{ref} = 1$ ) and all cost terms are defined as functions of  $C_{ref}$ . The multiplicative factor for initial cost ( $f_{ini}$ ) is calculated from Eqs. (7) to (10).

In order to determine a consistent value for the cost of one right-of-way inspection, Zhou & Nessim [5], for reference, used a unit cost of an inline inspection (for corrosion) equal to about 1.8% of the reference cost. Inline inspection for corrosion requires specialized equipment, skilled staff and pumping outage. The cost of a surveillance inspection for mechanical damage is drastically lower, since it is usually done by a person who goes along the pipeline route by car, by motorcycle, by bicycle or on foot. Thus, a multiplicative factor for inspection cost ( $f_{insp}$ ) of  $10^{-4}$  is adopted in this study. Again, pipeline operators could use a more specific number to reproduce the results presented in this article. Variation of total inspection cost with surveillance interval is shown in Figure 7.

Multiplicative factors for mechanical damage failure cost ( $f_{fail}$ ) are determined based on unit costs presented by Zhou & Nessim [5]. The cost of a failure is assumed to be the cost of excavating and repairing the damaged pipeline segment, the cost of property damage, and the compensation payoffs for injuries and death. The cost of fatality and injury can be determined from the values of a statistical life (VSL) and a statistical injury (VSI). Viscusi & Aldy [25] carried out a comprehensive review of published studies concerning mortality and injury risk premiums. The VSL values compiled by these authors exhibited large variations, which shows the need for evaluating the influence of VSL on the life-cycle cost optimization problem considered herein.

Different consequence scenarios are considered in this paper. Two parameters are varied to generate such different scenarios, namely the expected number of fatalities and VSL. Numbers of fatalities considered herein vary from one to five. Eighteen different VSL's, in the interval [18.63, 124.21] (dimensionless), taken from Viscusi & Aldy [25], are investigated. Failure factors ( $f_{fail}$ ) resulting from such considerations range from 61 to 664. In presenting numerical results, VSL's in monetary units are divided by the reference cost in order to make VSL dimensionless.

The multiplicative factor for repair cost ( $f_{rep}$ ) is also considered. The cost of a repair is assumed to consist of the cost of excavating and repairing the damaged pipeline segment. This results in  $f_{rep} = 0.135$ . In Eq. (21), an impact frequency ( $\omega$ ) of 0.004 per km·year [23] was used, and a repair frequency ( $\omega_{rep}$ ) of 0.5 was assumed. In spite of these considerations, it is important to mention that in the numerical study, the repair cost term was found to have a relatively minor influence on the objective function, Equation (24). Thus, the chosen values for  $f_{rep}$ ,  $\omega$  and  $\omega_{rep}$  have no great influence on the results.

The annual discount rate ( $\gamma$ ), which is used for inspection, failure and repair costs, is taken equal to 0.03. This value is in accordance with values cited by Wen [26] for public sector considerations.

Lower and upper bounds for the design variables are needed to solve the optimization problem. Such bounds were defined based on the ranges of validity [18] of Figures 1, 4 and 5. Additionally, the constraint  $D \leq 120 w_t$  is imposed [23]. For the pipeline analyzed in this paper, combining Eq. (5) and an approximate version of Eq. (4) with  $D_i \cong D$ , the above constraint leads to  $D \leq 650$  mm, approximately. Hence, the design variable bounds considered in this problem are  $[D^{\min}, D^{\max}] = [219.1, 650]$  mm,  $[h^{\min}, h^{\max}] = [0.5, 3]$  m, and  $[\Delta_s^{\min}, \Delta_s^{\max}] = [1, 28]$  days.

Although the curves shown in Figs. 1 to 5 are considered herein for evaluating failure rates and failure rate reduction factors, the problem formulation presented herein is generic and allows other curves to be considered. This also applies to the empirical cost of excavation curve, Eq. (9), and cost of inspections arbitrarily chosen.

An initial attempt to solve the optimization problem using mathematical programming algorithms showed the existence of multiple local minima. To circumvent such problems, an exhaustive search was employed in the present paper. In the exhaustive search, the objective function is evaluated at a fixed grid of design variable values. Then, the optimal objective function is chosen as the minimum among all the evaluated values. A grid of  $41 \times 201 \times 865$  points in  $(D \times h \times \Delta_s)$  was considered. The exhaustive search is a suitable method to solve this problem because objective function evaluations have negligible computational costs, as failure rates are estimated using Figs. 1 to 5 and applying Eq. (2).

## 4.2 Results

Solution of the optimization problem shows that all design variables depend on cost of failure scenarios, as shown in Table 2. The optimal external diameters are quite large, following the trend in Figure 1. This result shows that operators should favor large diameters: the larger initial costs are compensated by smaller failure rates, hence smaller expected costs of failure. Interestingly, for higher costs of failure, optimum diameters are reduced; this occurs due to increases in depth of cover and surveillance intervals.

For most cost of failure scenarios considered herein, the optimal depth of cover is equal to 2.25 m, which corresponds to the beginning of an almost flat region in Fig. 4. From this depth of cover on, the failure rate reduction factor becomes constant. Since the excavation cost continues to rise for  $h > 2.25$  m, and there is no compensation in terms of failure rate reduction,  $h = 2.25$  m is the optimum depth of cover. This depth of cover is deeper than the usual, frequently used 1.5 m. Note, however, that due to difficulties in quantifying its cost, we did not consider failure rate reduction for mechanical protection [18]. Only for  $C_{fail} = 61$  the optimal depth of cover was found to be 0.5 m.

Figure 8 shows the objective function in terms of  $D$  for fixed  $h = 2.25$  m and  $\Delta_s = 28$  days. It can be observed that total expected costs vary significantly with  $D$ , for all values of  $C_{fail}$ . It is clear that very small diameters lead to higher total expected costs, because of higher failure rates. Note that  $h = 2.25$  m and  $\Delta_s = 28$  days are non-optimal for  $C_{fail} = 61$  and  $C_{fail} = 602$ ; hence for these costs Fig. 8 only shows local minima.

Figure 9 shows the objective function in terms of  $h$  and  $\Delta_s$  for fixed  $D = 600$  mm and  $C_{fail} = 602$ . Figure 10 shows a cut of Fig. 9 for fixed  $\Delta_s = 4$  days and  $C_{fail} = 602$ , but also for other  $C_{fail}$  values. It can be observed that for the smaller costs of failure, total expected costs are mostly insensitive to depth of cover. However, for higher failure costs, total expected costs become sensitive w.r.t. depth of cover. For most values of  $C_{fail}$ , minimal total expected costs are obtained for  $h = 2.25$  m (Table 2).

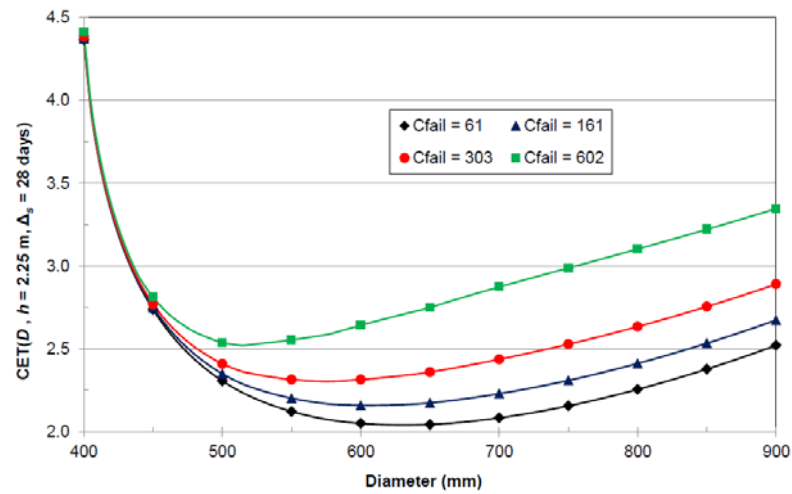


Figure 8 - Objective function for different external diameters and failure costs, for fixed depth of cover and surveillance interval.

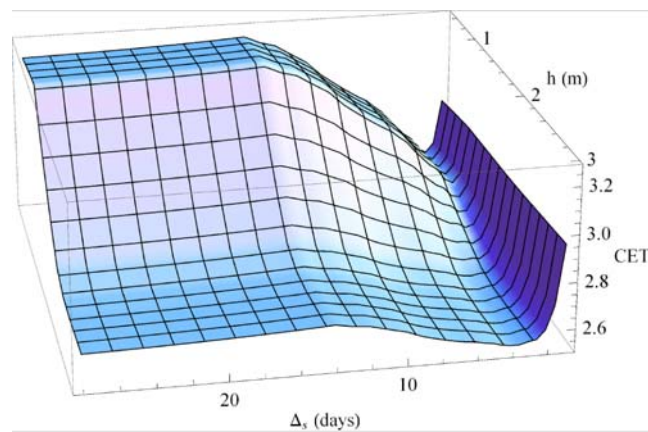


Figure 9 - Objective function in terms of  $h$  and  $\Delta_s$  for fixed  $D = 600$  mm and  $C_{fail} = 602$ .

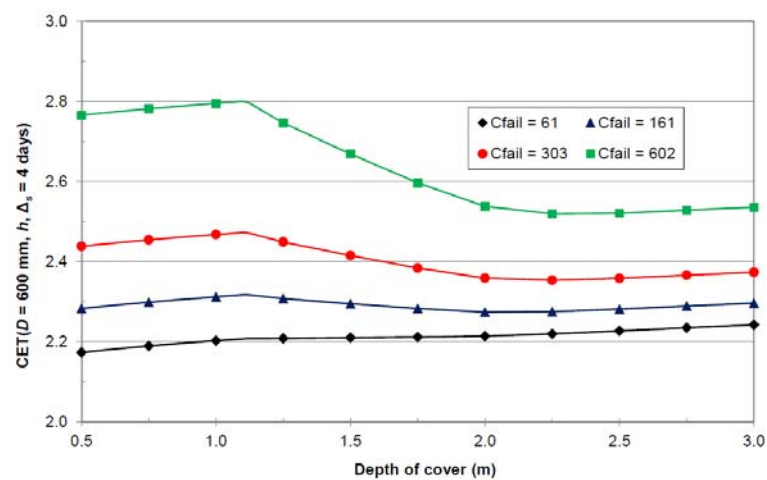


Figure 10 - Objective function for different depths of cover and failure costs, for fixed external diameter and surveillance interval.

Table 2: Optimal values of design variables in terms of cost of failure ( $f_{fail}$ ).

$f_{fail}$	$D^*$ (mm)	$h^*$ (m)	$\Delta_s^*$ (days)	$F_{obj}^*$
61	620	0.50	28	2.033
161	605	2.25	28	2.159
303	575	2.25	28	2.303
602	575	2.25	4.125	2.507

In analyzing the objective function (total expected cost,  $C_{ET}$ ), it was noted that the total inspection cost ( $C_{insp\_tot}$ ) decreases with increasing surveillance interval ( $\Delta_s$ ), as expected; however, this decrease is less pronounced for large surveillance intervals than for small ones. In particular, for values of  $\Delta_s$  greater than  $\approx 7$  days,  $C_{insp\_tot}$  varies slowly. This trend is illustrated in Fig. 7, and is important to understand the objective function behavior. On the other hand, the failure rate ( $\lambda_f$ ), which is directly proportional to the reduction factor for surveillance interval ( $R_{si}$ ), according to Eq. (2), increases with increasing  $\Delta_s$ , resulting in an increase of the failure cost term in  $C_{ET}$ ; however, this increase is not so pronounced for large  $\Delta_s$  values (Fig. 5). The failure cost term, of course, also increases with increasing  $C_{fail}$  according to Eq. (17).

Figure 11 shows the objective function for fixed  $D = 600$  mm and  $h = 2.25$  m, for different surveillance intervals and failure costs. The curve for  $C_{fail}=602$  is a cut of Fig. 9 for  $h = 2.25$  m. For small failure costs ( $C_{fail} \leq 303$ ) and for  $\Delta_s$  greater than about 7 days, it is observed that total expected costs are mostly insensitive to surveillance interval. For small failure costs, the decrease of  $C_{insp\_tot}$  with increasing  $\Delta_s$  governs the  $C_{ET}$  behavior for all values of  $\Delta_s$ . The failure cost term in the objective function increases with increasing  $\Delta_s$ , but this increase is not large enough to control  $C_{ET}$ . Thus, the minimal  $C_{ET}$  corresponds to the largest surveillance interval, i.e.  $\Delta_s = 28$  days.

For  $C_{fail}=602$ , total expected costs are more sensitive w.r.t. surveillance interval, and two local minima are clearly observable in the objective function (Fig. 11). The local minimum of  $\Delta_s=28$  days leads to higher total expected costs. The actual minimum is  $\Delta_s \approx 4$  days. The usual surveillance interval of  $\Delta_s=15$  days is actually a point of local maxima for this objective function. Significantly, the reduction in total expected costs, with respect to the local maxima of  $\Delta_s=15$  days, is around 5% for  $C_{fail}=602$ . The three different behaviors of the objective function, for large costs of failure, can be understood with reference to Figs. 5 and 7. For  $\Delta_s$  smaller than about 7 days, the pronounced decrease of  $C_{insp\_tot}$  results in reduction of  $C_{ET}$ . For  $\Delta_s$  between about 7 and 14 days, the slow reduction of  $C_{insp\_tot}$  makes the increasing failure cost term (increasing  $\lambda_f$ ) more important, which results in an increasing  $C_{ET}$  in this range. For  $\Delta_s$  greater than about 14 days, the increase of failure costs becomes less pronounced, and this results in greater influence of decreasing  $C_{insp\_tot}$ . Thus, for failure costs greater than about 400, the global optimum is not  $\Delta_s = 28$  days, but  $\Delta_s \approx 4$  days. Figure 12 further illustrates the issue, by presenting optimal  $\Delta_s$  in terms of fatalities and VSL values. It can be observed that for most values of VSL and for more than two potential fatalities, optimal surveillance interval is around 4 days. For very small VSL and for a single potential fatality, optimal surveillance interval is around 28 days.

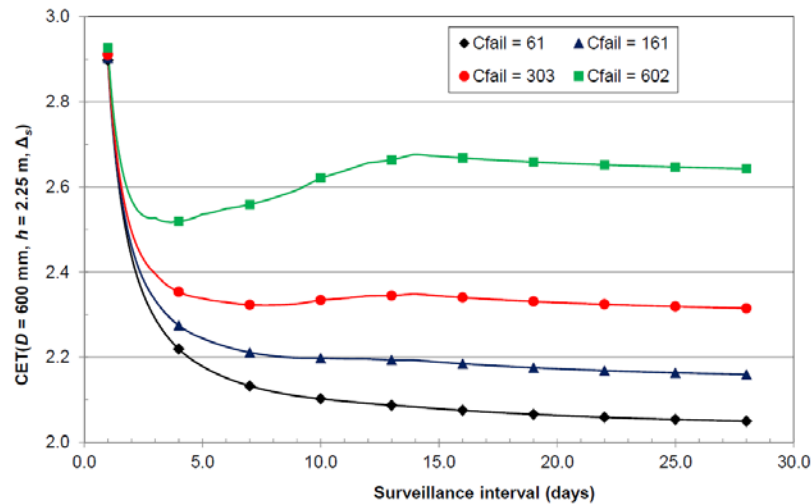


Figure 11 - Objective function for different surveillance intervals and failure costs, for fixed external diameter and depth of cover.

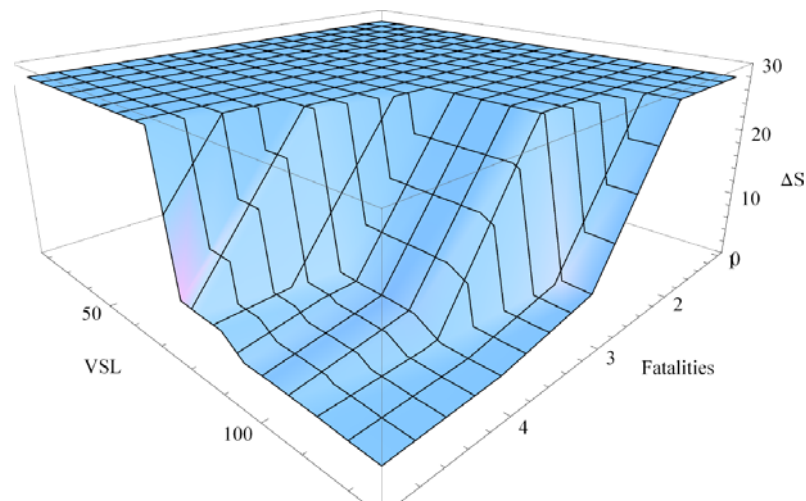


Figure 12 - Optimal surveillance interval for different numbers of fatalities and values of a statistical life.

## 5. CONCLUDING REMARKS

This paper addressed optimal design of buried onshore pipelines considering failure by mechanical damage. The curves controlling estimated failure rates w.r.t. different problem parameters were taken from UK design code PD8010:2009 [18]. Total expected life-cycle costs were minimized with respect to three problem parameters: external diameter, depth of cover and surveillance interval. Total expected life-cycle costs included the costs for fabrication and trench digging (burial), cost of right-of-way surveillance, cost of repairs and costs of failure.

Different costs of failure scenarios were considered, for different values of the Value of a Statistical Life (VSL) and potential number of fatalities. Results were found to be dependent on the actual cost functions. In general, however, it can be concluded that pipeline operators should favor larger pipe diameters and greater depth of cover. The study shows that the greater initial costs are fully compensated



by diminishing expected costs of failure. Interestingly, for larger costs of failure, optimal diameters are smaller, because failure rates are kept under control by deeper burial and more frequent surveillance.

The study also shows that optimal surveillance intervals are largely dependent on costs of failure (VSL and potential number of fatalities). For small costs of failure, surveillance interval could be of 28 days. For intermediate to large costs of failure, the customary 15-day surveillance interval actually leads to local maxima of total expected costs. For very large costs of failure, the surveillance interval could be reduced to 4 days, for a reduction of around 5% in total expected costs, in comparison to the customary 15 days.

## ACKNOWLEDGEMENTS

Sponsorship of this research project by the São Paulo Research Foundation - FAPESP (grant number 2012/11587-0) is gratefully acknowledged.

## REFERENCES

- [1] EGIG (2008). 7th EGIG-report 1970-2007: Gas Pipeline Incidents, European Gas Pipeline Incident Data Group, Groningen, Netherlands.
- [2] CONCAWE (2011). Performance of European cross-country oil pipelines: Statistical summary of reported spillages in 2009 and since 1971, Report n° 3/11 Brussels, Belgium.
- [3] UKOPA (2011). 8th Report of the UKOPA Fault Database Management Group: Pipeline Product Loss Incidents (1962-2010), United Kingdom Onshore Pipeline Operator's Association, Ambergate, UK.
- [4] Hong, H.P. (1999). Inspection and maintenance planning of pipeline under external corrosion considering generation of new defects, *Structural Safety* 21, 203–222.
- [5] Zhou, W., & Nessim, M.A. (2011). Optimal design of onshore natural gas pipelines, *Journal of Pressure Vessel Technology* 133, 031702-1–031702-11.
- [6] Gomes, W.J.S., Beck, A.T., & Haukaas, T. (2013). Optimal inspection planning for onshore pipelines subject to external corrosion, *Reliability Engineering and System Safety* 118, 18-27.
- [7] Gomes, W.J.S. & Beck, A.T. (2014). Optimal inspection and design of onshore pipelines under external corrosion process, *Structural Safety* 47, 48-58.
- [8] Beck, A.T. & Gomes, W.J.S. (2012). A comparison of deterministic, reliability-based and risk-based structural optimization under uncertainty, *Prob. Engineering Mechanics* 28, 18-29.
- [9] Beck, A.T., Gomes, W.J.S. & Bazán, F.A.V. (2012). On the robustness of structural risk optimization with respect to epistemic uncertainties, *International Journal for Uncertainty Quantification* 2, 1-20.
- [10] Nessim, M.A. & Zhou, W. (2009). Guidelines for reliability based design and assessment of onshore natural gas pipelines, C-FER Technologies, project n° L177, Final report submitted to Pipeline Research Council International, Inc., Edmonton, Canada.
- [11] Chen, Q. & Nessim, M.A. (1999). Reliability-based prevention of mechanical damage to pipelines, in: *Proc. 12th Biennial PRCI/EPRG Joint Technical Meeting on Pipeline Research*, Groningen, Netherlands.
- [12] Cosham, A. & Hopkins, P. (2001). A new industry document detailing best practices in pipeline defect assessment, in: *5th International Onshore Pipeline Conference*, Amsterdam, Netherlands.
- [13] Cosham, A. & Hopkins, P. (2002). The pipeline defect assessment manual, in: *Proc. IPC 2002 International Pipeline Conference*, Calgary, Canada, IPC02-27067.
- [14] Cosham, A. & Hopkins, P. (2004). The effect of dents in pipelines – guidance in the pipeline defect assessment manual, *International Journal of Pressure Vessels and Piping* 81, 127-139.
- [15] Macdonald, K.A. & Cosham, A. (2005). Best practice for the assessment of defects in pipelines – gouges and dents, *Engineering Failure Analysis* 12, 720-745.



- [16] Francis, A., Jandu, C.S., Andrews, R.M., Miles, T.J. & Chauhan, V. (2005). Development of a new limit state function for the failure of pipelines due to mechanical damage, in: Proc. 15th Biennial PRCI/EPRG Joint Technical Meeting on Pipeline Research, Orlando, USA.
- [17] Goodfellow, G.D., Haswell, J.V., McConnell, R. & Jackson, N.W. (2008). Development of risk assessment code supplements for the UK pipeline codes IGE/TD/1 and PD 8010, in: Proc. 7th International Pipeline Conference, Calgary, Canada, ASME, IPC2008-64493.
- [18] PD8010:2008, Code of practices for pipelines – Part 3: Steel pipelines on land – Guide to the application of pipeline risk assessment to proposed developments in the vicinity of major accident hazard pipelines containing flammables – Supplement to PD 8010-1: 2004, 2008.
- [19] Corder, I. (1995). The application of risk techniques to the design and operation of pipelines, in: Proc. International Conference on Pressure Systems: Operation and Risk Management, London, UK, Institution of Mechanical Engineers, 113-125.
- [20] Corder, I. & Chatain, P. (1995). EPRG recommendations for the assessment of the resistance of pipelines to external damage, in: Proc. 10th Biennial PRCI/EPRG Joint Technical Meeting on Pipeline Research, Cambridge, UK.
- [21] Cosham, A., Haswell, J.V. & Jackson, N. (2008). Reduction factors for estimating the probability of failure of mechanical damage due to external interference, in: Proc. 7th International Pipeline Conference, Calgary, Canada, ASME, IPC2008-64345.
- [22] Mather, J., Blackmore, C., Petrie, A. & Treves, C. (2001). An assessment of measures in use for gas pipelines to mitigate against damage caused by third party activity, WS Atkins Consultants Ltd for the Health and Safety Executive, Contract Research Report 372/2001, Birchwood UK.
- [23] CSA Z662:2007, Oil and gas pipeline systems, Canadian Standard Association, Mississauga, Ontario, Canada.
- [24] Fox, R.W., McDonald, A.T. & Pritchard, P.J. (2004). Introduction to fluid mechanics, sixth ed., John Wiley & Sons, Hoboken, USA.
- [25] Viscusi, W.K. & Aldy, J.E. (2003). The value of a statistical life: a critical review of market estimates throughout the world, *The Journal of Risk and Uncertainty* 27, 5-76.
- [26] Wen, Y.K. (2001). Minimum lifecycle cost design under multiple hazards, *Reliability Engineering and System Safety* 73, 223-231.